Reaction Intermediates and Molecular Mechanism of Peroxynitrite Activation by NO-Synthases

Jérôme Lang*[&], Amandine Maréchal[&], Manon Couture* and Jérôme Santolini[§]
From the iBiTec-S; C. E. A. Saclay; 91191 Gif-sur-Yvette Cedex; FRANCE
** From the Department of Biochemistry, Université Laval, Québec, Canada.*
[&] Both authors contribute equally to this article

Running title: Elucidating the controversial nature of the reaction intermediate

[§] Corresponding author: Santolini Jérôme, Ph. D. *Laboratoire de Stress Oxydant et Détoxication, iBiTec-S and CNRS URA 2096, C. E. A. Saclay - 91191 Gif-sur-Yvette Cedex – France.* Tel : 33-169085363; Fax : 33-169088717; E-Mail : jerome.santolini@cea.fr

ABSTRACT

The activation of peroxynitrite (PN) by hemoproteins, which leads to its detoxification or on the contrary to the enhancement of its cytotoxic activity, is a reaction of physiological importance that is still poorly understood. It has been known for some years that the reaction of hemoproteins, notably cytochrome P450, with PN leads to the build-up of an intermediate species with a Soret band at ~435 nm (I435). The nature of this intermediate is however debated. On the one hand, I435 has been presented as a Compound-II species that can be photo-activated to Compound I. A competing alternative involves the assignment of I435 to a ferric-nitrosyl species. Alike the cytochromes P450, the build-up of I435 occurs in NO-synthases (NOSs) upon their reaction with excess PN. Interestingly, the NOS isoforms vary in their capacity to detoxify/activate PN although they all show the build-up of I435. To better understand PN activation/detoxification by heme proteins, a definitive assignment of I435 is needed. Here we used a combination of fine kinetic analysis under specific conditions (pH, PN concentrations and PN/NOSs ratios) to probe the formation of I435. These studies revealed that I435 is not formed upon homolytic cleavage of the O-O bond of PN but that it arises from side-reactions associated with excess PN. Characterization of I435 by resonance Raman spectroscopy allowed its identification as a ferric iron-nitrosyl complex. Together, our study indicates that the model used so far to depict PN interactions with hemo-thiolate proteins, *i.e.* leading to the formation and accumulation of Compound II, needs to be reconsidered.

INTRODUCTION

The interaction between peroxynitrite (PN) and hemoproteins is one of the key-aspect to understand the biochemical fate and the biological activity of PN *in vivo [1-3]*. This is particularly true for NO-synthases (NOSs) that are the primary source of PN, and probably their primary target [4]. We recently highlighted the complexity of this interaction that can alternatively lead to the detoxification of PN or to the enhancement of its cytotoxic effect [5].

The reaction between PN and hemoproteins has been investigated for more than fifteen years [6-10]. The series of work devoted to hemo-thiolate proteins, such as NOS and cytochrome P450, showed the recurrent formation of an intermediate species with a Soret absorption around 432 - 440 nm (named **I435** through this manuscript) that is associated with an increase of the nitration potency of PN [4, 9, 11, 12]. This led to a commonly accepted mechanism that involved the homolytic cleavage of the PN O-O bond and the release of nitrogen dioxide ($NO_2°$, Scheme 1 – red arrows) with the concomitant build-up of a reaction intermediate identified as an oxoferryl species. This intermediate was later assigned to a Compound II species (Cpd-II) by Newcomb and colleagues when analyzing the interaction of PN with various cytochromes P450s [13-16]. This putative Cpd-II generated by the reaction of various P450 with PN was photoreduced to an intermediate that was somewhat competent for catalysis [15, 17]. The assignment of **I435** to Cpd-II was however contested by Green and coworkers who

proposed that the **I435** intermediate was an iron-nitrosyl complex[18].
In this regard we also raised concerns about the mechanism of PN activation by hemo-thiolate proteins. We have initiated a study of the interaction of PN with various NOS isoforms [5]. Not surprisingly, our results have proven so far to be quite similar to the ones obtained for CYPs [8, 9, 12, 19], and various peroxidases [7] [20]. Indeed, all NOS

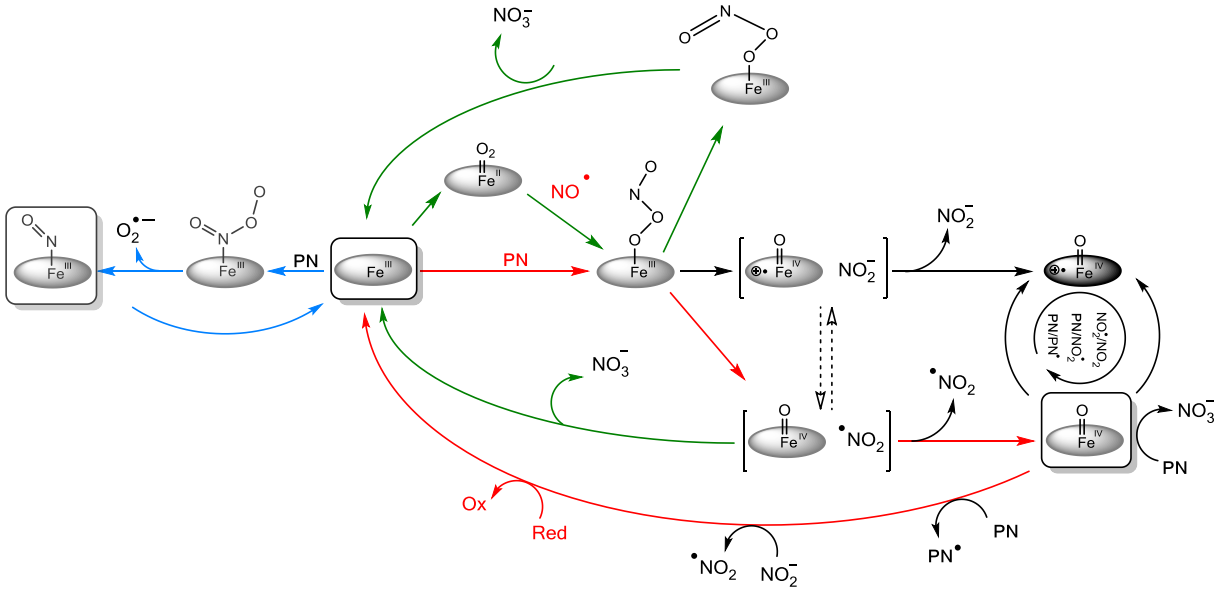

Scheme 1. Various reaction pathways for the decomposition of peroxynitrite by hemoproteins. Scheme 1 gives an example of the large diversity of redox reactions that might take place during the interaction of excess peroxynitrite with hemoproteins. Red arrows represent the pathway that has been proposed for peroxynitrite activation by hemo-thiolate proteins such as cytochromes P450. Green arrows represent the pathway for NO dioxygenation and peroxynitrite isomerization by globins. Blue arrows show a pathway involving the reactions from N-bound peroxynitrite (see Main Text for references).

isoforms showed the same build-up of the **I435** intermediate upon reaction with PN [4]. However, the outcome of this reaction varies among NOSs; from isomerization of PN, which releases nitrate, to PN activation, which releases NO_2°. This apparent absence of relationship between the observed nitration pattern by PN and the build-up of the **I435** intermediate raises the question of the nature of this intermediate.
This work aims to clarify the current debate on the nature of the **I435** intermediate and the molecular mechanism of PN activation by hemo-thiolate proteins. For this purpose, we combined two complementary approaches: i) a fine kinetic analysis focusing on the early phases of the reaction and on some important reaction conditions (pH, PN concentrations, PN/NOS molar ratios) and ii) characterization of the **I435** intermediate by using a T-mixer device for its formation coupled to resonance Raman spectroscopy for detection.
Resonance Raman spectroscopy is a very appropriate technique to characterize **I435**. It is a sensitive probe of the oxidation, coordination and spin states of the heme as well as to the nature of the heme axial ligands [21, 22]. Notably, the identity of a particular heme ligand can be validated using isotopic substitution. In NOSs, the proximal ligand involves the sulfur atom of a cysteine while the distal ligand would be O_2, or one of its derived activated states such as oxy-ferryl, as well as other usual heme ligands such as CO and NO.
By obtaining the time-resolved resonance Raman spectrum of **I435** in conditions directly comparable to those used for stopped-flow experiments, our results suggest that this intermediate is not an oxoferryl complex but rather an iron-nitrosyl complex as first suggested by Green and coworkers. Together, the results from these kinetic and spectroscopic studies indicate that the model that has been used so far to depict PN/hemo-thiolate interactions must be reconsidered.

EXPERIMENTAL PROCEDURES

Chemicals – All chemicals were purchased from Sigma or Aldrich Chemical Corp. (Sigma-Aldrich, St. Louis, MO, USA) except dihydrorhodamine (DHR) and rhodamine that were purchased from Calbiochem (EMD Biosciences, Inc., San Diego, CA, USA) and peroxynitrite (PN) that was purchased from Cayman Chemical (Cayman, Ann Arbor, MI, USA). PN solutions (between 37 and 45 µM in

NaOH 0.3 M) were stored as small (50-100 µL) aliquots at –80°C. Immediately before each experiment, PN concentration was measured by UV-visible spectroscopy (ε = 1670 $M^{-1}cm^{-1}$ at 302 nm). Argon (Ar) gas was purchased from Messer (Messer France SA, Asnières, France and Paxair, Canada). Nitric oxide was from Praxair, Canada.

Enzyme preparation – Wild-type iNOS oxygenase domains (iNOSoxy) containing a six-histidine tag at its C-terminus was expressed in *E. Coli* BL21 using the PCWori vector as already described [23, 24]. saNOS was expressed from the cloned gene in frame with a C-terminal six-histidine tag [25]. All proteins were purified in the absence of tetrahydrobiopterin (H_4B) and L-arginine (Arg) using Ni^{2+}-nitrilotriacetate affinity chromatography as reported previously[23, 25, 26]. iNOS concentration was determined by the absorbance at 444 nm of the heme ferrous-CO complex ($Fe^{II}CO$; ε_{444} = 74 $mM^{-1}.cm^{-1}$ [27]). saNOS concentration was determined from the pyridine-hemochrome method [28].

Stopped-flow experiments – iNOSoxy and saNOS were incubated in the absence of Arg and H_4B in a fresh anaerobized 100 mM KPi, 300 µM DTPA degassed buffer at the desired pH value. PN solutions were prepared shortly before use by diluting a fresh stock solution in anaerobized NaOH 0.01 N. Enzyme solutions were rapidly mixed to with PN solutions at 20°C. The mixing sequence gave a set of final concentrations of PN and NOSs. The pH of such solutions was verified after mixing and only negligible variations were noticed. Rapid-sampling stopped-flow experiments with $iNOS_{oxy}$ were performed on a Biologic (Bio-Logic Science Instruments SA, CLAIX, France) SFM 300 instrument coupled *via* a fiber optic cable with a Tidas spectrograph (WPI Inc., Sarasota, FL, USA) equipped with a rapid-sampling 1024 diode array detector (3 ms/spectrum). The light source was a 150 W Xe lamp. The spectral range of the monochromator was set from 200-1015 nm and the spectral resolution was 2 nm (0.8 nm/diode). Wavelength accuracy is quoted by the manufacturer to be 0.1 nm. A total of 750 UV-visible optical absorption spectra were recorded at various time intervals to encompass the whole kinetic reactions (3 and 40 seconds range). The apparatus dead-time was estimated to be less than 2 ms. The stopped-flow apparatus used to characterize the reaction of saNOS with PN is described in Supporting Information. The above protocol was adapted to the following types of experiments.

Kinetics of PN decay – These kinetics were investigated using a protocol similar to the one previously used for iNOSoxy [4]. PN decay was followed by the variations in absorbance at 302 nm in the presence of 1.5 µM iNOSoxy and with increasing concentrations of PN (10, 20, 50, 100, 200 µM). Three different experiments were recorded for each concentration. Several traces of the time-dependent variation in absorbance at 302 nm were multi-fitted to mono-exponential functions using the Origin 6.0 software routine (OriginLab Corporation, Northampton, MA, USA). This protocol was repeated three times. The apparent rate constants thus obtained were averaged and plotted as a function of PN concentrations. The kinetics of PN decay catalyzed by saNOS at various PN concentrations were followed at 302 nm. The experimental details and the results are described in the Supporting information (Fig. S3).

Kinetic analysis of heme spectral transitions – A 100 µM solution of PN was rapidly mixed with 4 µM of iNOSoxy at three different pHs (6.4, 7.4 and 8.4). This reaction was monitored at wavelengths characteristic of specific species and/or events depending on pH conditions, such as PN decay (302 nm), the ferric state of $iNOS_{oxy}$ (419 - 423 nm for the Soret band and 624 nm for the charge-transfer band) and the catalytic intermediate **I435** (441 - 447 nm). UV-visible absorption spectra were extracted from spectra *vs* time data sets at specific times to highlight defined transitions phases and to reveal complete PN consumption. These spectra correspond to the initial and final states those at maximal concentration of intermediate(s). Difference absorption spectra were calculated from the initial and intermediate spectra to characterize the nature and extent of spectral changes at specific time points.

Kinetics of build-up and decay* of *I435– Time-dependent traces of the variation in absorbance at 445 nm were used to determine the time (t) at which the maximal concentration of iNOSoxy intermediate **I435** was reached, *i.e.* between 200 to 300 ms, depending on the experimental conditions. The UV-Visible absorption spectrum of the intermediate **I435** was systematically calculated by subtracting from the spectrum at (t) an estimated fraction

that remained of the initial spectrum. This allowed us to estimate the wavelength maximum of the Soret band for intermediate **I435** for each condition of pH and PN concentration. The apparent rates of build-up and decay of the intermediate **I435** were obtained by analyzing the time-dependent traces of the increase (from 0 to 250 ms) and decrease (from 400 ms to the end of the kinetics) in absorption at this specific wavelength. These traces were fitted to a mono-exponential function to obtain apparent rates of build-up and decay. The same experiment has been achieved at several pHs from 6.2 to 8.4 and with 10-200 µM PN concentrations. The reported rates of build-up and decay of iNOSoxy **I435** correspond to the average of three independent experiments. The kinetics of build-up and decay of **I435** were also characterized using saNOS and various concentrations of PN. The data were fitted to a global three-state model involving the initial ferric enzyme (state A), **I435** (state B) and final low-spin ferric (state C) states. The experimental details and the results appear in as Supporting information (Fig. S1, S2 and S3).

Stoichiometric reaction of iNOSoxy with PN – A 60 µM PN solution was rapidly mixed with 60 µM iNOSoxy at 4 °C. The solutions were prepared to ensure a final pH of 7.4 after mixing. Superimposed spectra were analyzed to characterize heme spectral transitions. These were characterized by the presence of clear isobestic points.

Resonance Raman characterization of reaction intermediates during early- and steady-state phases – To further characterize intermediate **I435**, a continuous-flow mixer [29] was used to obtain its resonance Raman spectrum in the high- and low-frequency regions. The resonance Raman spectra were acquired at 94 ms after mixing saNOS (50 µM) with PN (5 mM), in 100 mM KPi buffer pH 6.4 + 300 µM DTPA which corresponds to the time at which the maximal concentration of intermediate **I435** was reached (Supplementary Fig. S1). The final pH of such mixed solution did not exceed 7.3. The equilibrium reference spectra of the Fe^{III} and $Fe^{III}NO$ complexes of saNOS were obtained in a Raman cell that was kept spinning to avoid local heating of the samples. The excitation wavelengths were the 413.133 nm line of a Kr laser (Fe^{III}) and the 441.563 nm line of a He/Cd laser ($Fe^{III}NO$ and **I435**).

The early phase of the reaction of saNOS with PN was probed 2.5 ms after mixing. Since **I435** had not accumulated to a significant extent at such a short time after mixing, the optical spectrum had a Soret near that of the initial ferric state as determined from the stopped-flow kinetic data. Accordingly, the 413.133 nm line of a Kr laser was used to acquire the resonance Raman spectrum in the early-phase in the high-frequency region.

RESULTS

Effect of pH on the kinetics of build-up of the I435 intermediate. A100 µM PN solution was rapidly mixed using a stopped-flow apparatus with 4 µM iNOSoxy in a degassed 0.1 M KPi buffer of pH values ranging from 6.2 to 8.4. Experimental and analytical procedures are the same as the ones described previously [4] (see Experimental Procedures). We observed, for each pH value, the build-up of the same intermediate that we and other teams previously described [4, 5]. The reconstructed absorption spectra of this **I435** intermediate exhibited an apparent absorption maximum that shifted from 439.5 nm at pH 6.2 to 446 nm at pH 8.4 (not shown). All of the reconstructed spectra exhibited similar Q-band features at 547-48 and 585-88 nm indicating that a similar intermediate species was being observed. We noted that the extent of **I435** build-up, and its lifespan, significantly decreased as the pH increased.

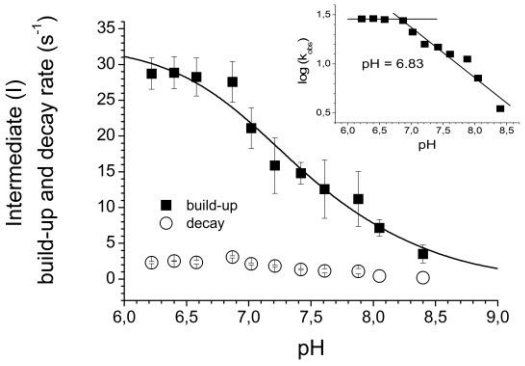

Figure 1: Analysis of the pH-dependence of the apparent rates of I435 build-up and decay. A 100 µM PN solution was rapidly mixed with 4 µM iNOSoxy at 20 °C at pHs ranging from 6.2 to 8.4. The kinetic traces were fitted to a mono-exponential function to obtain the apparent rates of build-up and decay of I435. These apparent rates were plotted as a function of pH. Inset: The logarithmic plot of the rates of I435 build-up vs pH was fitted to a simple model assuming one acido-basic couple with a pKa ~6.8.

Kinetic traces showing **I435** build-up and decay were monitored at the wavelength of **I435** maximal absorption and were fitted to a mono-exponential function to get the apparent

rates of these transitions. The apparent rate constants were then plotted as a function of pH (Fig. 1, filled square). The rate of **I435** decay was clearly pH independent. In contrast, the rate of **I435** formation increased upon acidification of the solution up to a plateau. This behavior is characteristic of the involvement of an acido-basic equilibrium. The apparent pKa this transition was estimated at pH 6.8 from the logarithmic plot (Fig. 1, inset). Our results clearly suggest that the build-up of **I435** involves at least one acido-basic equilibrium. They also suggest that protonated peroxynitrite (PNH) is the actual reactive species.

Effect of PN Concentration on the Kinetics of Formation of the Intermediate I435 and on the Kinetics of decomposition of PN. Aliquots of increasing concentrations of PN (from 12.5 to 200 μM final concentration) were rapidly mixed with iNOSoxy (1.5 μM final concentration) in a degassed 0.1 M KPi buffer at pH 7.4. Stopped-flow experimental and analytical procedures were the same as described above. The spectral characteristics of the resulting intermediate **I435** were the same for every PN concentration, i.e. the wavelength maximum of the Soret band was centered at *ca.* 443 nm (data not shown).

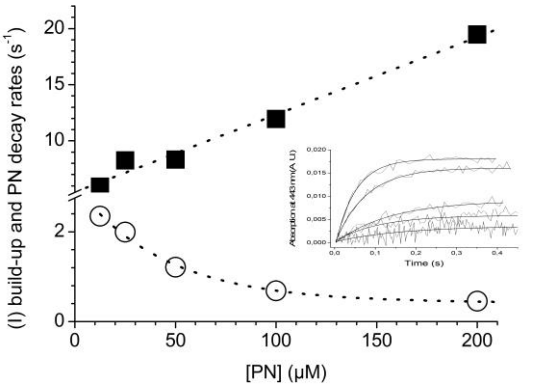

Figure 2: Analysis of PN concentration-dependence of the rates of I435 build-up and PN decay. Various concentrations of PN were rapid-mixed with 1.5 μM iNOSoxy in a freshly anaerobized KPi buffer at pH 7.4. Conditions as described under Experimental Procedures. Time traces recorded at 443 nm (representative of **I435** build-up) were fitted to a mono-exponential function. The apparent rate constants were then plotted as a function of PN concentration for **I435** build-up (filled square) and for PN decay (open circle). Inset: The kinetic traces recorded at 443 nm that show the build-up of the intermediate **I435** for the same increasing PN concentrations as the main figure.

Kinetic traces of **I435** build-up (Fig. 2, inset) were fitted to a mono-exponential function and the observed rate constants were plotted as a function of PN concentration (Fig. 2, main). The apparent rate of **I435** formation increased linearly with the concentration of PN. The second order rate constant calculated from these data was $6.9 \pm 0.5 \times 10^4$ $M^{-1}s^{-1}$ at pH 7.4. This linear relationship indicates that a bimolecular reaction of PN with iNOSoxy controls the kinetics of formation of the intermediate **I435**. We also determined the kinetics of PN decomposition for increasing concentrations of PN (between 10 and 200 μM) by analyzing directly PN decay at 302 nm. The kinetic traces were fitted to a mono-exponential function and the apparent rate constants were plotted as a function of PN concentration (Fig. 2, open circles). The rate of PN decomposition decreased as PN concentration increased, which is consistent with the larger extent of buildup of I435 detected at higher PN concentrations (Fig. 2, insert). As the PN concentration increased, the rate of **I435** formation increased but that of PN decay decreased, suggesting that distinct pathways characterize **I435** build-up and PN decay.

Stoichiometric reaction of PN with iNOSoxy. We then analyzed the profile of PN decomposition at stoechiometric PN/iNOSoxy ratio. A solution of 60 μM PN was rapidly mixed with a solution of 60 μM iNOSoxy at pH 7.4 using the same procedure described above (see Experimental procedures). PN decayed relatively rapidly with an apparent rate constant of 7.8 s^{-1}, compared to 0.1 s^{-1} in the absence of iNOSoxy, which indicates that the vast majority of PN was decomposed as it reacted with iNOSoxy (Not shown). This apparent decay rate constant matches the one calculated using PN activation rate (k_{act} = 6.3±0.6 s^{-1} [4]).

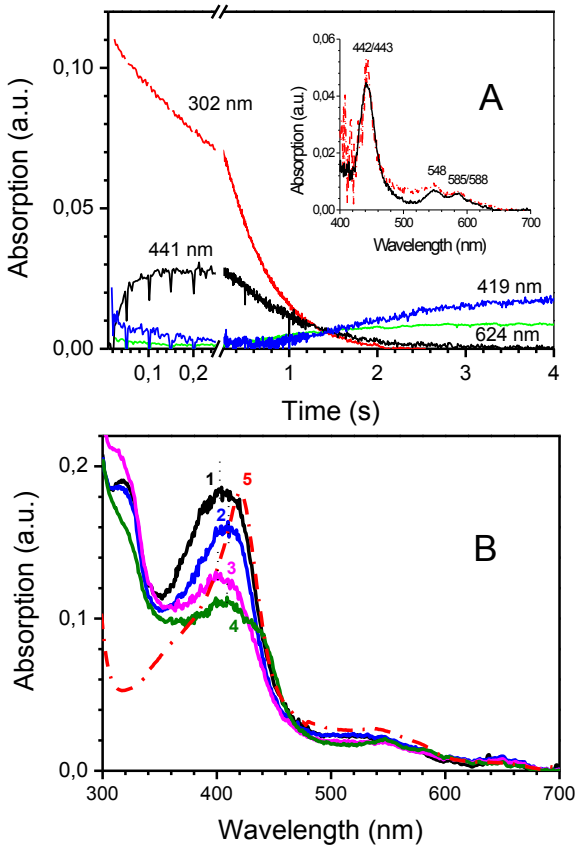

Figure 3: Kinetic phases observed during PN activation by iNOSoxy at pH 6.4. A 100 µM PN solution was rapidly mixed with 4 µM iNOSoxy in a KPi 0.1 M pH 6.4 buffer at 20 °C. Conditions as described under Experimental Procedures. Panel A. Main: The kinetic traces showing the variation in absorbance at characteristic wavelengths: 302 nm (red), 419 nm (blue), 441 nm (black), 624 nm (green). Inset: calculated spectra of intermediates detected for steady-state assays at pH 6.4 (black line) and for a reaction with a stoichiometric PN/iNOSoxy ratio at pH 7.4 (red line, see Experimental Procedures). Panel B. Superimposition of UV-visible absorption spectra that correspond to the successive intermediates observed during the early phase of PN activation by iNOSoxy at pH 6.4. Spectra at 3 ms (1), 12 ms (2), 21 ms (3), 201 ms (4) and 4.35 s (final) are shown.

Unlike what we observed under conditions of excess PN [4], only a small amount of the **I435** intermediate was observed (~7%, Fig. 3A, inset, red trace). This small build-up hints towards different mechanisms for PN decomposition between conditions of stoichiometric- and excess-PN.

Successive Kinetic Phases of iNOS-induced PN Activation. We previously reported the existence of two distinct kinetic phases for the heme spectral changes during iNOSoxy-induced PN activation at pH 7.4, characterized by the build-up and decay of the **I435** intermediate [4]. Since PN activation was faster at acidic pH [4], we investigated here the kinetics of iNOSoxy heme spectral changes at pH 6.4. Figure 3A shows the kinetic phases observed by stopped-flow optical absorption spectroscopy during activation of PN (100 µM) by 4 µM iNOSoxy in a degassed KPi buffer at pH 6.4 (see Experimental Procedures). Kinetic traces were monitored at characteristic wavelengths such as 302 nm (PN decay), 419 nm (ferric iNOS) and 441 nm (**I435**) and they suggest the existence of the same four phases that we reported at pH 7.4 [4]. The initial-, intermediate- and final-UV-visible absorption spectra are displayed in Fig. 3B. Unexpectedly, the initial UV-visible absorption spectrum of iNOSoxy obtained right after mixing with PN (3 ms, Fig. 3B, Spectrum 1) exhibited a broad Soret band (95 nm FWHM) with an apparent maximum centered around 404 nm and displayed an additional weak absorption at 650 nm, both of which are significantly different from the spectral features of native iNOSoxy, i.e. a wavelength maximum of the Soret band centered at ~419 nm (60 nm FWHM) and no absorption at 650 nm. The first observable kinetic phase (3 → 21 ms) is characterized by successive changes in the apparent wavelength maximum of the iNOSoxy Soret band (404→409→400 nm, spectra 2, 3) with a progressive loss in absorption intensity (greater than 20 %). The second phase (up to 200 ms) is characterized by the partial decay of the absorption at 318 nm and the concomitant build-up of an intermediate characterized by a shoulder around 445 nm and the absence of the absorption band at 650 nm (Fig. 3B, Spectrum 4). The third and fourth phases are similar to the ones described at pH 7.4 and correspond to the disappearance of the shoulder at 445 nm (up to 1.5 s) followed, after the complete consumption of PN, by a modification of ferric iNOSoxy that then displayed a Soret band centered at 411 nm and a new absorption band at 624 nm (data not shown).

The major intermediate species observed at pH 6.4 have very similar spectra features compared to the ones previously described at pH 7.4 [4]. However, we notice here the presence of several additional intermediate complexes in the initial phase of PN activation, which suggests an intricate interplay between iNOSoxy and PN that might involve different acido-basic forms of PN and heme intermediates.

Characterization by Resonance Raman Spectroscopy of the intermediate(s) formed during the early- and steady-state phases of PN activation. To gain insight into the nature of the **I435** intermediate and the early

intermediate(s), we turned to resonance Raman spectroscopy coupled with a rapid T-mixer to generate and probe these intermediates. Due to the large amount of protein required to carry out continuous-flow experiment [29], we used the bacterial NOS-like enzyme of *Staphylococcus aureus*, saNOS, which is well suited for those experiments and has been well characterized previously by steady-state and time-resolved resonance Raman spectroscopy [30, 31]. We first measured the apparent rate of PN decay achieved for iNOSoxy using this new model. The kinetics of **I435** build-up and decay were characterized as well. Stopped-flow optical spectroscopy experiments of the reaction of saNOS and PN show the transient build-up on a time-course of ~100 ms of intermediate **I435**. Global analysis revealed that the time-course of the overall reaction is characterized by main spectral contributions from three species which were the initial ferric state (Soret band at 398 m, mainly high-spin heme), **I435** (Soret band centered at 440 nm) and the final ferric state (Soret band centered at 418, mainly low-spin heme) (Supplementary Fig. S1). The analysis of the early phase of the reaction (1.5 to 12 ms) revealed a first optical transition characterized by an isosbestic point near 430 nm that is distinct from the isosbestic point at 423 that corresponded to the later formation of **I435** (Supplementary Fig. S2). The detection of these two isosbestic points indicate that reactions other than the build-up of **I435** take place in the early phase of the reaction of saNOS with PN. The kinetics of PN decay followed at 302 nm show that saNOS accelerates the decomposition of PN (Supplementary Fig. S3). As described for iNOSoxy, the rates of build-up and decay of **I435,** and the decay of PN, followed distinct patterns of dependence with respect to the concentration of PN (Supplementary Fig. S3). This whole profile, similar to that reported for bsNOS [5] and here with iNOSoxy, confirms that the properties of the reaction with PN are shared by all these NOSs and validates the use of saNOS to characterize **I435**. We then used resonance Raman spectroscopy coupled with a continuous flow T-mixer to characterize the **I435** intermediate and to trap and identify any new reaction intermediates in the early phase of PN activation. The resonance Raman spectrum of the intermediate **I435** was recorded in the high-frequency region 94 ms after mixing ferric saNOS (50 µM) with PN (5 mM) to probe the heme core modes (See Experimental Procedures for the details). Figure 4A shows the resonance Raman spectra obtained for the PN/saNOS mixture (corresponding to **I435**), for the equilibrium $Fe^{III}NO$ species and for the native ferric enzyme. Notably, the ν_4 line of **I435** (1376 cm^{-1}) was shifted by 3 cm^{-1} with respect to that of the ferric resting enzyme (1373 cm^{-1}) and was nearly identical to that of the $Fe^{III}NO$ complex of saNOS (1375 cm^{-1}). In the 1470-1510 cm^{-1} region, the ν_3 lines characteristic of the 5C high-spin state (1489 cm^{-1}) and of the 6C low-spin state (1503 cm^{-1}) were detected in the spectrum of ferric resting saNOS as reported previously [25]. In the spectrum of **I435,** the ν_3 line at 1489 cm^{-1} that arises remaining ferric heme was much less intense and a new line centered at 1504 cm^{-1} was apparent.

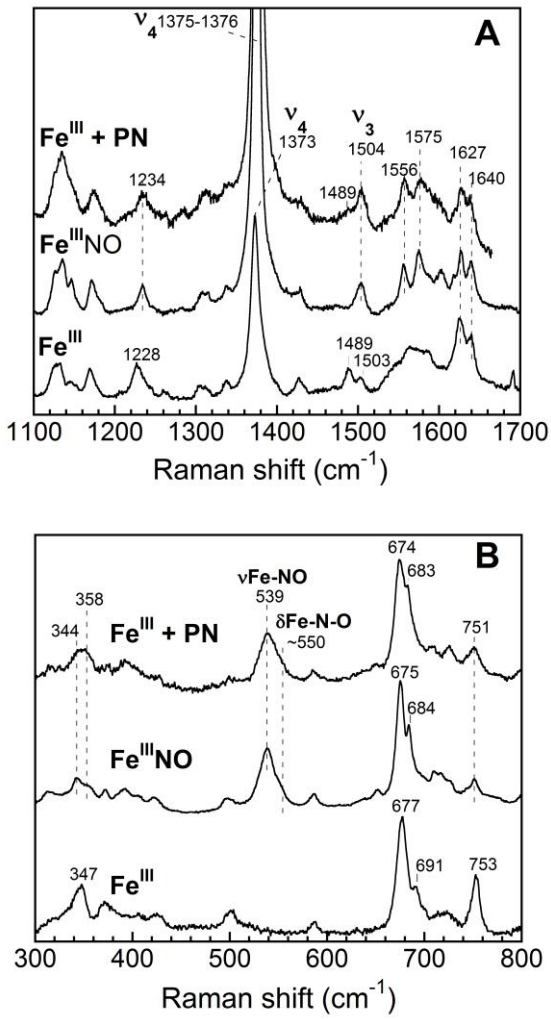

Figure 4: Resonance Raman spectra of Intermediate I435. High-frequency- (A) and low-frequency regions (B) of the resonance Raman spectrum of the intermediate **I435** recorded 94 ms after mixing ferric saNOS with PN (Fe^{III} + PN). The equilibrium reference spectra of saNOS in the ferric (Fe^{III}) and $Fe^{III}NO$ states are also shown. The excitation wavelengths were 441.563 nm ($Fe^{III}NO$ and Fe^{III} + PN) and 413.133 nm (Fe^{III}).

This new ν_3 line displayed a frequency identical to that of the ν_3 line of the $Fe^{III}NO$ complex [31]. Additionally, the 1556 cm^{-1} (ν_{11}) and 1575 cm^{-1} (ν_2) lines of the $Fe^{III}NO$ complexes, which are not apparent in the resting Fe^{III} spectrum, are observed in the spectrum of **I435**. Overall, these results indicate that the heme core modes of **I435** are very similar to those of the $Fe^{III}NO$ complex of saNOS.

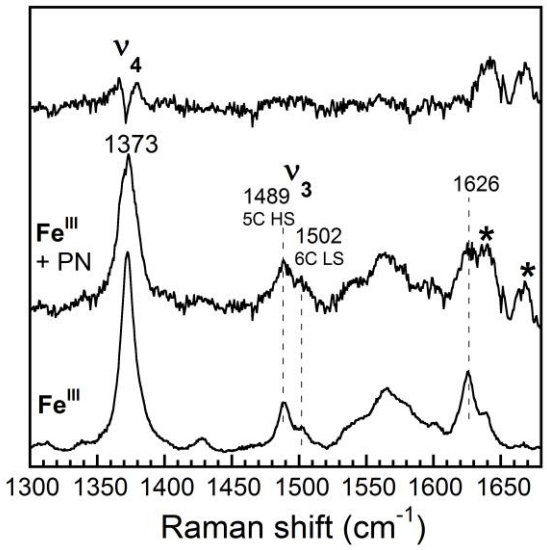

Figure 5: Analysis by resonance Raman spectroscopy of the early intermediate(s). The resonance Raman spectrum of the early intermediate(s) was acquired in the high-frequency region 2.5 ms after mixing ferric saNOS with PN. The excitation wavelength was 413.133 nm. The spectrum of ferric saNOS is shown as a reference. The difference spectrum calculated from these spectra is also shown (top trace)

I435 was probe in the low-frequency region to obtain further evidence about its identity. The low-frequency region of resonance Raman spectra contains vibrational lines that provide information about the heme axial ligands as well as other lines that arise form in- and out-of-the plane porphyrin vibrations [21, 22]. An intense line centered at 539 cm^{-1} was detected in the spectrum of **I435** along with a shoulder near 550 cm^{-1} (Fig. 4B). A very intense line and a shoulder at the same frequencies were observed previously in the low-frequency region of the spectrum of the $Fe^{III}NO$ complex of saNOS and were assigned to the $\nu_{Fe\text{-}NO}$ mode (539 cm^{-1}) and $\delta_{Fe\text{-}N\text{-}O}$ (553 cm^{-1}) mode, respectively, based on the isotope shifts [32]. No other heme complex of saNOS is known to display such intense lines at these frequencies (half the intensity of ν_8 at 674 cm^{-1}). The Fe-OO mode of the oxygenated state of saNOS is at 517 cm^{-1} and its intensity is very small [29]. The frequency of the Fe-O stretching mode of the Cpd-II state was never reported for this protein. Such mode would be expected at a much higher frequency (near 790-800 cm^{-1}) given the double-bond character of the Fe=O bond of an unprotonated ferryl state such as that of horseradish peroxidase [33, 34] and myoglobin [35, 36]. If a putative Cpd-II of saNOS was protonated, like that of chloroperoxidase [37], the frequency could be near 565 cm^{-1}, which is almost 30 cm^{-1} higher than the $\nu_{Fe\text{-}NO}$ mode of saNOS. Other porphyrin lines at 683/684 and 751 cm^{-1} of **I435** and $Fe^{III}NO$ have nearly identical frequencies and they are clearly different from those of the ferric resting saNOS spectrum (691 and 753 cm^{-1}) (Fig. 4). Overall, the similarities of the porphyrin modes of **I435** and of the $Fe^{III}NO$ complex, in both the high- and low-frequency regions, along with the detection of the intense $\nu_{Fe\text{-}NO}$ and $\delta_{Fe\text{-}N\text{-}O}$ modes in the time-resolved spectrum strongly indicates that **I435** is a $Fe^{III}NO$ complex.

We repeated this experiment but recorded the resonance Raman spectrum at 2.5 ms after mixing to probe the early phase the reaction of saNOS with PN. In this condition, the resonance Raman spectrum obtained in the high-frequency region was nearly identical to that of resting ferric saNOS (Fig. 5). This is consistent with the fact that **I435** had not accumulated to a significant extent at that time as revealed from the stopped-flow data (Supplementary Fig. S1, Panel E). The ν_3 and ν_4 region of the 2.5 ms spectrum (saNOS + PN) and that of ferric saNOS show a similar mixture of high- and low-spin states, which is reflected in the nearly flat difference spectrum calculated with these spectra (Fig. 5). The optical spectra recorded at 1.5-12 ms after mixing saNOS with PN display a slight blue-shift with respect to the ferric resting state (Supplementary Fig. S2). As describe above, a clear isosbestic point, different from the one that characterizes the build-up of **I435,** is also observed in the early-phase of the reaction. Although these results suggest the formation of an early intermediate, resonance Raman spectroscopy failed to detect its spectral fingerprints possibly because this intermediate did not accumulate to a level high enough to allow its detection.

DISCUSSION

Kinetic Analysis of the Interaction between PN and NO-Synthases. The interaction of PN with hemo-thiolate proteins has been the focus of numerous reports in the last twenty years.

Analysis of such reactions by stopped-flow optical spectroscopy and steady-state assays [7, 9] led to evidence of the build-up of a heme complex that display spectroscopic fingerprints similar to those of the chloroperoxidase Compound II (Cpd-II) complex. The interaction of PN with various hemo-thiolate proteins consistently led to an increased in the level and complexity of the nitration pattern of PN, suggesting the release of nitrogen dioxide, $NO_2°$ [11]. As consequence, the simplest model to account for these observations proposed that the reaction of PN with hemo-thiolate proteins results in the homolytic cleavage of the PN O-O bond leading to a [Cpd-II $NO_2°$] caged pair (Scheme 1, red arrows). However, several pieces of information suggest that the observed reactions might not directly correspond to the sole activation of PN by the heme.

First, the kinetics of PN/NOS interaction seem to change depending on the molar ratio between PN and NOS. In conditions that were standardly used in previous reports, *i.e.* when PN is in excess (100 µM PN for 2 µM NOS) we observed (here and in previous reports[4]) a strong build-up of the **I435** intermediate. However, using a stoichiometric PN/NOS ratio, we did observed the strong acceleration of PN decay but only negligible **I435** build-up. Reciprocally, as the PN concentration increased, we observed that the extent and rate of **I435** build-up increased whereas the rate of PN decay decreased. This divergent pattern suggests that at least two modes of PN decomposition might co-exist: one fast mode at low PN/iNOSoxy molar ratio that does not necessarily involve **I435** formation, and one slow mode at high PN/iNOSoxy molar ratio that leads to **I435** build-up.

The fast mode corresponds likely to the reaction of PN with the NOS ferric heme and does not seem to engage **I435** buildup. The slow mode is characterized by the build-up of the **I435** intermediate and might involve additional side-reactions of PN with other heme intermediates or with RNS end-products. This hypothesis of multiple PN decomposition routes has been already envisioned for metallo-porphyrins [38] and metallo-proteins [1]. Cross-reactions of PN with the Compound I- or Compound II intermediates [39-42] [43] but also iron-oxo [44-47] and iron-nitrosyl complexes [42, 48, 49] have been commonly proposed.

Thus, the activation of PN - as seen by the acceleration of its decay – is not univocally linked to **I435** formation, which, in turn, could correspond to reaction intermediates different from oxoferryl species.

Nature of the NOS intermediate I435 observed during the activation of PN. The nature of the **I435** intermediate has been from the beginning the key element for proposing the mechanism of interaction of PN with hemo-thiolate proteins. In this regard, the similarity between the spectroscopic fingerprints of **I435** and oxoferryl complexes has led the first research groups to assign this reaction intermediate to a Cpd-II-like species [12, 13]. More recently Newcomb and coworkers used X-Ray absorption spectroscopy to identify the reaction intermediate observed upon interaction of PN with cytochrome P450 as a Cpd-II species [13]. The photo-oxidation of this intermediate apparently gave rise to the build-up of a Cpd-I species [14, 17, 50, 51], alike what was reported for chloroperoxidase [16]. Such species showed some competency for substrates oxidation reinforcing the first assignment of **I435** as an oxoferryl intermediate. Moreover, the Newcomb's group recently reported a similar kinetic behavior for a putative Cpd-I generated with m-chloroperoxybenzoic acid and for that obtained from the photoreduction of **I435** generated by the reaction with PN [52]. However, this dual assignment (Cpd-I and Cpd-II complexes) was challenged by Green and coworkers. Indeed, the Green's group did not observe the same spectroscopic fingerprints for the Cpd-I species of P450 [53, 54]. Second, using Mossbauer spectroscopy, they suggested that the initial **I435** intermediate would not be a Cpd-II but rather an iron-nitrosyl species. However, the differences in the Mossbauer parameters for all these compounds remain minor and in the absence of additional spectroscopic characterization of the **I435** intermediate, the dispute might go on [52, 55].

In this context, our report brings a novel and definitive piece of evidence concerning the nature of the **I435** intermediate. Using time-resolved resonance Raman spectroscopy and stopped-flow/UV-visible spectroscopy, **I435** was obtained and probed in the same experimental conditions, and can thus be directly compared. We did not observe any signal corresponding to an oxoferryl complex at the reaction time corresponding to maximal **I435** build-up. Instead, the frequencies of the porphyrin vibrational modes and the strong ν_{Fe-N} vibrational mode are the clear signature of a

$Fe^{III}NO$ species. As resonance Raman spectroscopy is one of the best suited method to probe NO coordination to hemoproteins, our results strongly indicate that the **I435** intermediate is most likely to be a $Fe^{III}NO$ complex. Our results also indicate that such a complex arises from secondary reactions involving excess PN. In this environment, the $Fe^{III}NO$ complex is not stable and decays back to the ferric state within seconds suggesting that **I435** disappearance may be linked to other secondary reactions as well. How photoreduction of such a complex mixture may trap a Cpd-I state at relatively high-yield is not clear [52, 55]. Beyond the dispute between the Newcomb's and Green's groups concerning the spectroscopic fingerprints of Cpd-I and Cpd-II complexes, the major outcome of our work concerns the reaction of PN with hemoproteins and the link between PN activation and **I435** intermediate formation. In this regard, our results call into question the current mechanism, which proposes that **I435** formation arises from the homolytic cleavage of PN O-O bound.

Relationship between PN activation and build-up of the I435 intermediate. NOS isoforms represent a good investigative model of the reaction of PN with hemoproteins. Indeed, despite the similar 3D structure of their catalytic site, they exhibit different interaction profiles with PN. Although all NOSs undergo reactions that result in the build-up of intermediate **I435**, these reactions when looked at biochemically lead either to an enhanced nitration pattern by PN (iNOS) or to the scavenging of PN (bsNOS) [5]. The reason why the same proposed mechanism of activation, that involves PN homolytic cleavage and $NO_2°$ release, could lead to different outcomes for PN reactivity has remained unexplained so far.

Our results indicate that the build-up of **I435**, which is $Fe^{III}NO$ complex, is not the landmark of PN homolytic cleavage and the formation of a [Cpd-II / $NO_2°$] cage pair. Thus the persistent build-up of **I435** observed for all NOSs might be related to side-reactions, whereas the reactions that truly correspond to PN activation – and that remain unexplored - might differ among NOS isoforms.

The mechanism of activation of heme-bound PN can be derived from former investigations that concern the reactions of NO dioxygenation by oxyhemoglobin [56]. Indeed, this reaction is believed to lead to a heme-bound PN complex, that will eventually undergo a homolytic cleavage, leading to the formation of a [Cpd-II / $NO_2°$] cage pair. This step would be followed by a direct recombination of $NO_2°$ on the oxoferryl complex, resulting in the isomerization of PN and the release of nitrate [57] (Scheme 1, green arrow). The formation of PN-heme complex is believed to take place within 1 ms of PN interaction with the heme [58] and might in fact even be too fast to be observed [59].

In the case of NOSs (and other hemo-thiolate proteins), these reactions should even be faster giving the greater reactivity of their heme conferred by the elevated electronic "push" capacity from the thiolate bond. Thus the intermediates involved in PN activation by NOSs might be too transient to be observed. Our stopped-flow results are consistent with this proposal; the first- and other early-spectroscopic fingerprints seem to indicate that a sequence of reactions had already taken place within the dead-time of our rapid-mixing device and in the first milliseconds of the observed kinetics. This may indicate that the first observed optical absorption spectrum does not correspond to the native resting enzyme and that the homolytic cleavage reaction may already be completed. However the time-resolved resonance Raman investigation of the initial kinetic event(s) only revealed the presence of the porphyrin modes characteristic of the ferric species and did not show any additional feature that may originate from intermediates. It may be that these intermediates do not accumulate to a sufficiently level to be detected.

Formation and decay of a $Fe^{III}NO$ complex. As we demonstrated that the **I435** intermediate does not arise directly from the homolytic cleavage of the PN O-O bond, the question of its formation arises. There are two possible scenarios: *i) an alternative mechanism of PN decomposition*. In this scenario, PN binds to the native heme but the active intermediate would correspond to a N-bound PN complex that could experience an homolytic N-O bond cleavage leading to the formation of $Fe^{III}NO$ (Scheme 1, blue arrows) and the release of superoxide anion ($O_2°^-$). The dissociation rate of free PN ($NO/O_2°^-$,[60]) has been estimated to be around 0.017 s^{-1}, which is far below the rates of PN decay observed in these experiments (between 0.1 and 2 s^{-1} depending on the conditions). Thus one could conceive that heme speeds up the cleavage of the N-O bond of PN, accounting for the increased rate of PN decomposition. *ii) NO rebinding*. In this

second scenario, PN decomposition through various paths will eventually lead to the accumulation of NO as a side-product that will bind to free heme and shift the steady-state equilibrium towards the transient accumulation of $Fe^{III}NO$. There are almost no observations related to these hypotheses, and further experiments are required to help understand the mechanism of formation of a heme-NO complex out of PN decomposition.

Conclusion. Our results unambiguously show that the crucial intermediate observed in the reaction of PN and hemo-thiolate proteins, believed to be a Compound II species, is not an oxoferryl complex but a $Fe^{III}NO$ complex. Its build-up is not linked to the homolytic cleavage of the PN O-O bond but arises from side-reactions associated with the presence of excess of PN. The enhanced nitration patterns resulting from heme-induced PN activation is disconnected from **I435**/$Fe^{III}NO$ build-up. New experiments and concepts are now needed to investigate the details of PN activation mechanism. In this regard, NO-synthase isoforms represent a good model to correlate the mechanism of O-O bond activation and the biological fate of PN.

SUPPORTING INFORMATION

Supplementary Fig. S1. Global analysis using a three-state model (A→B→C) of optical absorption spectra versus time data sets of the reaction of saNOS with PN.
Supplementary Fig. S2. Early-phase of PN activation by saNOS.
Supplementary Fig. S3 PN concentration-dependence of the apparent rates of **I435** build-up and decay, and of the apparent rate of PN decay, that are catalyzed by saNOS.

AUTHOR CONTRIBUTIONS

JS and MC planned experiments; JL, AM, JS and MC performed experiments; AM, JL, MC, JS analysed data; MC and JS wrote the paper.

[1]The abbreviations used are: Arg, L-arginine; Cpd-I and Cpd-II, Compound I and II in chloroperoxidase and catalase catalytic cycle ; DHR, dihydrorhodamine; DTPA, diethylenetriaminepentaacetic acid; FAD, flavin adenine dinucleotide; FMN, flavin adenine mononucleotide; FNR, Ferredoxin-NADP-Reductase; $Fe^{II}NO$, ferrous heme-nitric oxide complex; $Fe^{III}NO$, ferric heme-nitric oxide complex; $Fe^{II}CO$, ferrous heme-carbon monoxide complex; H_4B, tetrahydrobiopterin, (6R)-5,6,7,8-tetrahydro-L-biopterin; Hb, hemoglobin; Mb, myoglobin; KPi, inorganic phosphate buffer; NADPH, Nicotinamide Adenine Dinucleotide Phosphate reduced form; NO, nitric oxide; NOHA, N^{ω}-hydroxy-L-arginine, NOS, nitric oxide synthase; NOSoxy, oxygenase domain of NOS; eNOS, endothelial nitric oxide synthase; iNOS, inducible nitric oxide synthase; nNOS, neuronal nitric oxide synthase; bsNOS, NOS-like protein isolated from *Bacillus subtilis*; saNOS, NOS-like protein isolated from *Staphylococcus aureus*, $P450_{BM3}$, cytochrome P450 CYP120 isolated from *Bacillus megaterium*; $P450_{Cam}$, camphor 5-monoxygenase isolated from *Pseudomonas putida*; PN, peroxynitrite anion; PNH, peroxynitrous acid; ROS, Reactive Oxygen Species; RNS, Reactive Nitrogen Species. 5C, 5-coordinate state of the heme; 6C, 6-coordinate state of the heme

REFERENCES

1. Herold, S. and A. Fago, *Reactions of peroxynitrite with globin proteins and their possible physiological role.* Comp Biochem Physiol A Mol Integr Physiol, 2005. **142**(2): p. 124-9.
2. Ferrer-Sueta, G. and R. Radi, *Chemical biology of peroxynitrite: kinetics, diffusion, and radicals.* ACS Chem Biol, 2009. **4**(3): p. 161-77.
3. Koppenol, W.H., et al., *Peroxynitrous acid: controversy and consensus surrounding an enigmatic oxidant.* Dalton Trans, 2012. **41**(45): p. 13779-87.
4. Marechal, A., et al., *Activation of peroxynitrite by inducible no-synthase : A direct source of nitrative stress.* J Biol Chem, 2007.
5. Marechal, A., et al., *NO synthase isoforms specifically modify peroxynitrite reactivity.* FEBS J, 2010. **277**(19): p. 3963-73.
6. Su, J. and J.T. Groves, *Mechanisms of peroxynitrite interactions with heme proteins.* Inorg Chem, 2010. **49**(14): p. 6317-29.

7. Gebicka, L. and J. Didik, *Kinetic studies of the reaction of heme-thiolate enzyme chloroperoxidase with peroxynitrite.* J Inorg Biochem, 2007. **101**(1): p. 159-64.
8. Floris, R., et al., *Interaction of myeloperoxidase with peroxynitrite. A comparison with lactoperoxidase, horseradish peroxidase and catalase.* Eur J Biochem, 1993. **215**(3): p. 767-75.
9. Mehl, M., et al., *Peroxynitrite reaction with heme proteins.* Nitric Oxide, 1999. **3**(2): p. 142-52.
10. Herold, S., et al., *Mechanistic studies of the isomerization of peroxynitrite to nitrate catalyzed by distal histidine metmyoglobin mutants.* J Am Chem Soc, 2004. **126**(22): p. 6945-55.
11. Daiber, A., et al., *The impact of metal catalysis on protein tyrosine nitration by peroxynitrite.* Biochem Biophys Res Commun, 2004. **317**(3): p. 873-81.
12. Daiber, A., et al., *Nitration and inactivation of cytochrome P450BM-3 by peroxynitrite. Stopped-flow measurements prove ferryl intermediates.* Eur J Biochem, 2000. **267**(23): p. 6729-39.
13. Newcomb, M., et al., *X-ray absorption spectroscopic characterization of a cytochrome P450 compound II derivative.* Proc Natl Acad Sci U S A, 2008. **105**(24): p. 8179-84.
14. Newcomb, M., et al., *Cytochrome p450 compound I.* J Am Chem Soc, 2006. **128**(14): p. 4580-1.
15. Sheng, X., et al., *Kinetics of oxidation of benzphetamine by compounds I of cytochrome P450 2B4 and its mutants.* J Am Chem Soc, 2009. **131**(8): p. 2971-6.
16. Yuan, X., et al., *Low temperature photo-oxidation of chloroperoxidase Compound II.* J Inorg Biochem, 2010. **104**(11): p. 1156-63.
17. Sheng, X., J.H. Horner, and M. Newcomb, *Spectra and kinetic studies of the compound I derivative of cytochrome P450 119.* J Am Chem Soc, 2008. **130**(40): p. 13310-20.
18. Behan, R.K., et al., *Reaction of cytochrome P450BM3 and peroxynitrite yields nitrosyl complex.* J Am Chem Soc, 2007. **129**(18): p. 5855-9.
19. Daiber, A., et al., *Autocatalytic nitration of P450CAM by peroxynitrite.* J Inorg Biochem, 2000. **81**(3): p. 213-20.
20. Gebicka, L. and J.L. Gebicki, *Reactions of heme peroxidases with peroxynitrite.* IUBMB Life, 2000. **49**(1): p. 11-5.
21. Spiro, T.G., A.V. Soldatova, and G. Balakrishnan, *CO, NO and O as Vibrational Probes of Heme Protein Interactions.* Coord Chem Rev, 2013. **257**(2): p. 511-527.
22. Rousseau, D.L., et al., *Ligand-protein interactions in nitric oxide synthase.* J Inorg Biochem, 2005. **99**(1): p. 306-23.
23. Ghosh, D.K., et al., *Inducible nitric oxide synthase: role of the N-terminal beta-hairpin hook and pterin-binding segment in dimerization and tetrahydrobiopterin interaction.* EMBO J, 1999. **18**(22): p. 6260-70.
24. Gachhui, R., et al., *Mutagenesis of acidic residues in the oxygenase domain of inducible nitric-oxide synthase identifies a glutamate involved in arginine binding.* Biochemistry, 1997. **36**(17): p. 5097-103.
25. Chartier, F.J. and M. Couture, *Stability of the heme environment of the nitric oxide synthase from Staphylococcus aureus in the absence of pterin cofactor.* Biophys J, 2004. **87**(3): p. 1939-50.
26. Adak, S., K.S. Aulak, and D.J. Stuehr, *Direct evidence for nitric oxide production by a nitric-oxide synthase-like protein from Bacillus subtilis.* J Biol Chem, 2002. **277**(18): p. 16167-71.

27. Stuehr, D.J. and M. Ikedasaito, *Spectral Characterization of Brain and Macrophage Nitric-Oxide Synthases - Cytochrome-P-450-Like Hemeproteins That Contain a Flavin Semiquinone Radical.* Journal of Biological Chemistry, 1992. **267**(29): p. 20547-20550.
28. Appleby, C.A., *Purification of Rhizobium cytochromes P-450.* Methods Enzymol, 1978. **52**: p. 157-66.
29. Chartier, F.J., S.P. Blais, and M. Couture, *A weak Fe-O bond in the oxygenated complex of the nitric-oxide synthase of Staphylococcus aureus.* J Biol Chem, 2006. **281**(15): p. 9953-62.
30. Chartier, F.J. and M. Couture, *Substrate-specific interactions with the heme-bound oxygen molecule of nitric-oxide synthase.* J Biol Chem, 2007. **282**(29): p. 20877-86.
31. Lang, J., et al., *Trp180 of endothelial NOS and Trp56 of bacterial saNOS modulate sigma bonding of the axial cysteine to the heme.* J Inorg Biochem, 2009. **103**(7): p. 1102-12.
32. Chartier, F.J. and M. Couture, *Interactions between substrates and the haem-bound nitric oxide of ferric and ferrous bacterial nitric oxide synthases.* Biochem J, 2007. **401**(1): p. 235-45.
33. Ikemura, K., et al., *Red-excitation resonance Raman analysis of the nu(Fe=O) mode of ferryl-oxo hemoproteins.* J Am Chem Soc, 2008. **130**(44): p. 14384-5.
34. Kincaid, J.R., et al., *Resonance Raman spectra of native and mesoheme-reconstituted horseradish peroxidase and their catalytic intermediates.* J Biol Chem, 1996. **271**(46): p. 28805-11.
35. Zeng, W., et al., *Synchrotron-derived vibrational data confirm unprotonated oxo ligand in myoglobin compound II.* J Am Chem Soc, 2008. **130**(6): p. 1816-7.
36. Behan, R.K. and M.T. Green, *On the status of ferryl protonation.* J Inorg Biochem, 2006. **100**(4): p. 448-59.
37. Stone, K.L., R.K. Behan, and M.T. Green, *Resonance Raman spectroscopy of chloroperoxidase compound II provides direct evidence for the existence of an iron(IV)-hydroxide.* Proc Natl Acad Sci U S A, 2006. **103**(33): p. 12307-10.
38. Crow, J.P., *Peroxynitrite scavenging by metalloporphyrins and thiolates.* Free Radic Biol Med, 2000. **28**(10): p. 1487-94.
39. Crow, J.P., *Manganese and iron porphyrins catalyze peroxynitrite decomposition and simultaneously increase nitration and oxidant yield: implications for their use as peroxynitrite scavengers in vivo.* Arch Biochem Biophys, 1999. **371**(1): p. 41-52.
40. Ascenzi, P., et al., *Peroxynitrite scavenging by ferryl sperm whale myoglobin and human hemoglobin.* Biochem Biophys Res Commun, 2009. **390**(1): p. 27-31.
41. Ascenzi, P., et al., *Peroxynitrite detoxification by ferryl Mycobacterium leprae truncated hemoglobin O.* Biochem Biophys Res Commun, 2009. **380**(2): p. 392-6.
42. Herold, S. and A. Puppo, *Kinetics and mechanistic studies of the reactions of metleghemoglobin, ferrylleghemoglobin, and nitrosylleghemoglobin with reactive nitrogen species.* J Biol Inorg Chem, 2005. **10**(8): p. 946-57.
43. Lee, J.B., J.A. Hunt, and J.T. Groves, *Mechanisms of iron porphyrin reactions with peroxynitrite.* J Am Chem Soc, 1998. **120**(30): p. 7493-7501.
44. Minetti, M., et al., *Scavenging of peroxynitrite by oxyhemoglobin and identification of modified globin residues.* Biochemistry, 2000. **39**(22): p. 6689-97.
45. Romero, N., et al., *Reaction of human hemoglobin with peroxynitrite. Isomerization to nitrate and secondary formation of protein radicals.* J Biol Chem, 2003. **278**(45): p. 44049-57.

46. Herold, S. and A. Puppo, *Oxyleghemoglobin scavenges nitrogen monoxide and peroxynitrite: a possible role in functioning nodules?* J Biol Inorg Chem, 2005. **10**(8): p. 935-45.
47. Exner, M. and S. Herold, *Kinetic and mechanistic studies of the peroxynitrite-mediated oxidation of oxymyoglobin and oxyhemoglobin.* Chem Res Toxicol, 2000. **13**(4): p. 287-93.
48. Herold, S. and F. Boccini, *NO* release from MbFe(II)NO and HbFe(II)NO after oxidation by peroxynitrite.* Inorg Chem, 2006. **45**(17): p. 6933-43.
49. Herold, S., *The outer-sphere oxidation of nitrosyliron(II)hemoglobin by peroxynitrite leads to the release of nitrogen monoxide.* Inorg Chem, 2004. **43**(13): p. 3783-5.
50. Yuan, X., et al., *Kinetics and activation parameters for oxidations of styrene by Compounds I from the cytochrome P450(BM-3) (CYP102A1) heme domain and from CYP119.* Biochemistry, 2009. **48**(38): p. 9140-6.
51. Wang, Q., et al., *Quantitative production of compound I from a cytochrome P450 enzyme at low temperatures. Kinetics, activation parameters, and kinetic isotope effects for oxidation of benzyl alcohol.* J Am Chem Soc, 2009. **131**(30): p. 10629-36.
52. Su, Z., J.H. Horner, and M. Newcomb, *Cytochrome P450 119 Compounds I Formed by Chemical Oxidation and Photooxidation Are the Same Species.* Chemistry, 2012.
53. Rittle, J. and M.T. Green, *Cytochrome P450 compound I: capture, characterization, and C-H bond activation kinetics.* Science, 2010. **330**(6006): p. 933-7.
54. Rittle, J., J.M. Younker, and M.T. Green, *Cytochrome P450: the active oxidant and its spectrum.* Inorg Chem, 2010. **49**(8): p. 3610-7.
55. Krest, C.M., et al., *Reactive intermediates in cytochrome p450 catalysis.* J Biol Chem, 2013. **288**(24): p. 17074-81.
56. Arnold, E.V. and D.S. Bohle, *Isolation and oxygenation reactions of nitrosylmyoglobins.* Nitric Oxide, Pt B, 1996. **269**: p. 41-55.
57. Blomberg, L.M., M.R. Blomberg, and P.E. Siegbahn, *A theoretical study of myoglobin working as a nitric oxide scavenger.* J Biol Inorg Chem, 2004. **9**(8): p. 923-35.
58. Olson, J.S., et al., *No scavenging and the hypertensive effect of hemoglobin-based blood substitutes.* Free Radic Biol Med, 2004. **36**(6): p. 685-97.
59. Yukl, E.T., S. de Vries, and P. Moenne-Loccoz, *The millisecond intermediate in the reaction of nitric oxide with oxymyoglobin is an iron(III)--nitrato complex, not a peroxynitrite.* J Am Chem Soc, 2009. **131**(21): p. 7234-5.
60. Goldstein, S., J. Lind, and G. Merenyi, *Chemistry of peroxynitrites as compared to peroxynitrates.* Chem Rev, 2005. **105**(6): p. 2457-2470.